Heliyon 10 (2024) e24617

Contents lists available at ScienceDirect

Heliyon

journal homepage: www.cell.com/heliyon

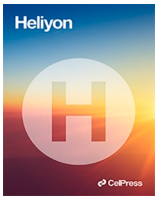

Research article

Anti-inflammatory effects of *Chrozophora plicata* uncovered using network pharmacology and in-vivo carrageenan paw edema model

Mohd Mukhtar Khan [a,d,*], Syed Ayaz Ali [a,d], Yasar Qazi [b,d], Subur W. Khan [c,d], Md Affan shaikh [b,d]

[a] *Department of Pharmacology, Y.B Chavan College of Pharmacy, Aurangabad, Maharashtra, India*
[b] *Department of Chemistry, Y.B Chavan College of Pharmacy, Aurangabad, Maharashtra, India*
[c] *Department of Pharmacognosy, Y.B Chavan College of Pharmacy, Aurangabad, Maharashtra, India*
[d] *Y.B Chavan College of Pharmacy, Dr Rafiq Zakaria Campus, Aurangabad, 431001, Maharashtra, India*

ARTICLE INFO

Keywords:
Inflammation
Carrageenan
Chrozophora plicata, network pharmacology
Molecular docking

ABSTRACT

Chrozophora plicata has been extensively utilized in India for the management of numerous disorders. The effective Phytoconstituents derived from the Ethyl Acetate Fraction of *Chrozophora plicata* [EAFCP] have been identified as Camptothecin Agathisflavone, Rutin, Procynidine B, and Apigenin. These Phytoconstituents have been detected in the EAFCP through qualitative analysis using LC-Q-TOF-MS/MS. The anti-inflammatory properties of *Chrozophora plicata* are yet to be determined. Therefore, the aim of this study was to utilize a network pharmacology-based methodology to predict potential therapeutic targets of EAFCP in the setting of inflammation. The identification of inflammation targets was followed by the acquisition of verified targets of EAFCP. The key therapeutic targets of EAFCP against inflammation were found by creating a target-functional PPI network, GO studies were conducted on the core therapeutic targets in order to assess the essential signalling pathways involved in the anti-inflammatory effects of EAFCP. A total of 38 significant hub targets associated with EAFCP's anti-inflammatory effects were identified. The key proteins were retrieved for the docking investigation based on the findings, which aided in anticipating the potential interaction between components and targets. The in vivo study revealed that EAFCP had a notable efficiency in decreasing paw edema induced by carrageenan in rats. The evidence we have gathered collectively offers clarification about the anti-inflammatory activity of EAFCP, which is predominantly linked to the suppression of the Cox 1, 2 pathway. The aforementioned findings highlight potential therapeutic targets that could be utilized for the anti-inflammatory activity of EAFCP.

1. Introduction

Inflammation is a fundamental aspect of the body's innate immunological response. Numerous chronic ailments, such as cancer, diabetes, cardiovascular illnesses, and autoimmune diseases, manifest as a result of tissue degradation and genetic modifications induced by enduring low-grade inflammation within the impacted tissue or organ. Inflammation is a multifaceted physiological

* Corresponding author. Y.B Chavan College of Pharmacy, Dr Rafiq Zakaria Campus, Aurangabad, 431001, Maharashtra, India.
E-mail address: mukhtarpharma@gmail.com (M.M. Khan).

https://doi.org/10.1016/j.heliyon.2024.e24617
Received 30 October 2023; Received in revised form 14 December 2023; Accepted 11 January 2024
Available online 2 February 2024

reaction that serves as a crucial component in the body's protective response against detrimental stimuli. Nevertheless, in cases when inflammation persists over a prolonged period or surpasses normal levels, it has the potential to give rise to a diverse array of incapacitating ailments, such as rheumatoid arthritis, asthma, and inflammatory bowel disease [1,2]. The pursuit of efficient anti-inflammatory medicines has emerged as a central focus in contemporary biomedical research. Natural products have historically served as a valuable resource for the exploration of novel drugs, and their ability to influence inflammatory responses has been extensively documented. *Chrozophora plicata* [CP], an indigenous traditional medicinal plant found in diverse places worldwide, has attracted considerable interest due to its alleged anti-inflammatory effects. Despite its long utilization in traditional medicine, there is still limited understanding of the exact pathways through which *CP* exerts its anti-inflammatory benefits in the context of contemporary pharmacology. The primary aim of this research investigation is to bridge the current gap in knowledge by employing a multidisciplinary approach that combines network pharmacology with in-vivo experimentation [3]. The current investigation aims to elucidate the pharmacological attributes of *Chrozophora plicata* via network pharmacology methodologies and in vivo assessments [4–6]. The primary objective is to discern and scrutinize the plausible anti-inflammatory mechanisms and pathways linked with the compounds inherent in *Chrozophora plicata*. The study further endeavours to gauge the efficacy of *Chrozophora plicata* in mitigating inflammation by employing the in-vivo Carrageenan Paw Edema model. Moreover, it seeks to establish a correlative relationship between the anticipated pharmacological actions and the observed anti-inflammatory effects witnessed in the animal model. Furthermore, our research has the potential to lay the foundation for the advancement of novel medications that are based on the ancient knowledge and principles of traditional medicine. In the context of a global population suffering from chronic inflammatory illnesses, the exploration of *Chrozophora plicata's* capacity to mitigate inflammation holds promise for the development of enhanced therapeutic approaches [7].

2. Material and methods

2.1. Plant selection and authentication

The plant was recognized and verified by the herbarium department of botany at Dr. Babasaheb Ambedkar Marathwada University, Aurangabad. A sample was kept with the department under voucher number 00732.

2.2. Preparation of ethyl acetate fraction of Chrozophora plicata

The foliage procured from the university campus underwent a meticulous drying process spanning 48 h. Upon complete desiccation, the leaves were pulverized. Utilizing Methanolic solvent (CAS No 67-56-1), the plant matter was subjected to continuous percolation using a Soxhlet apparatus for a duration of 72 h. The resultant extract was dissolved in water and subjected to treatment with ethyl acetate (CAS no 141-78-6) via a separating funnel for a period of 4–6 h. The ethyl acetate fraction retrieved was collected in petri dishes and subsequently exposed to open air for 24 h to achieved a defined state. This fraction was then dispatched to IIT Powai Mumbai for further analysis of its phytochemical composition using LCMS-QTOF, The methodology for LCMS-QTOF shown in (Supplementary Materials).

2.3. Phytochemical network and Disease-Target Network

Using binding.db.net and the structural similarity of 70 % with the following chemical ingredients, Agathisflavone, Apigenin 7-glucoside, camptothecin, procyanidin-B7, and rutin, the major phytochemical constituents in the plant were then evaluated for their target genes. The target genes and phytochemical components listed below were then visualized using a network created in cytoscape version 11.0.6. The following target genes were then analysed for their related diseases in Disgen.net and the diseases related to inflammation were screened and filtered furthermore the genes which had relation to inflammatory disease was noted and the edges and nodes of the target genes and inflammatory diseases was visualized by a constructing a network in cytoscape v11.0.6 [8–10].

2.4. PPI network and clue go analysis

The analysis of the target genes was conducted using the string v11.5 database, and the protein-protein interaction [PPI] network was constructed by applying a high confidence threshold of 0.7. The genes exhibiting the highest betweenness, centrality, and degree were identified and ranked using the cytohubba tool, which was employed for network analysis. The genes under investigation were next subjected to gene ontology analysis using Clue Go v2.5.9. A p-value threshold of 0.005 was applied to address the issue of false discovery rate, along with a moderate specific filter in the database. This analysis aimed to examine the functional aspects of biological processes [11]. The retrieval of biological processes, cellular components, Kegg pathways, and molecular characteristics was performed using the g Profiler plugin within the Cytoscape software [12–14].

2.5. Molecular docking

2.5.1. Software tools

Protein Data Bank (https://www.rcsb.org/) was used to retrieve the target proteins. The target proteins was optimized, purified,

and prepared for docking with the help of Discovery Studio Visualizer 2020 by removing unwanted water molecules, bound ligands from protein structure, and saved again in PDB file format to the same folder. The AutoDock Vina 1.1.2 in PyRx 0.8 was used to perform the docking studies of selected ligands and approved drug (Indomethacin). Results were analysed and visualized by PyMol software (The PyMOL Molecular Graphics System, Version 2.4.1 Schrödinger, LLC).

2.5.2. Ligand preparation

The structures (SDF File) of ligands and approved drug (Indomethacin) were downloaded from the official website of the U.S. National Library of Medicine PubChem (https://pubchem.ncbi.nlm.nih.gov/) Table 1. The structure was then imported into PyRx 0.8

Table 1
Core metabolites of *Chrozophora plicata*.

Name	PubChem CID	Structure
Agathisflavone	5281599	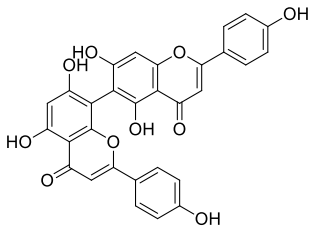
Apigenin	5280443	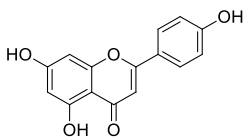
Camptothecin	24,360	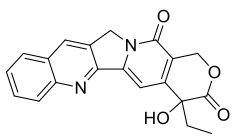
Procyanidine	107,876	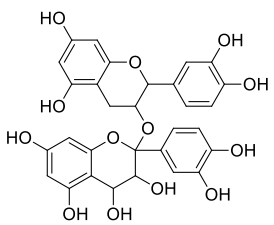
Rutin	5280805	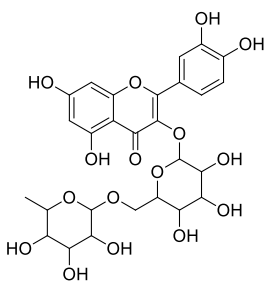

using open babel tool and energy minimization (optimization) was performed by considering fundamental parameters based on the element, its hybridization, and connectivity, i.e., by Universal Force Field. This ligand was then converted to AutoDock Ligand format (PDBQT).

2.5.3. Target preparation

The AutoDock Vina 1.1.2 in PyRx 0.8 was used to perform the docking studies of selected natural compounds and approved drug (Indomethacin) against the crystal structure of COX-1 and COX-2. The recently elucidated three-dimensional Crystal Structure of Cyclooxygenase-1 in complex with celecoxib (PDB: 3KK6) and Cyclooxygenase-2 in complex with celecoxib (PDB: 3LN1) was selected for the study. The crystal structure of 3KK6 (https://www.rcsb.org/structure/3KK6) and 3LN1 (https://www.rcsb.org/structure/3LN1) have been retrieved from the RCSB. The viral protein structure was optimized, purified, and prepared for docking with the help of Discovery Studio Visualizer 2020 by removing unwanted water molecules, bound ligands from protein structure, and saved again in PDB file format to the same folder.

2.5.4. Docking procedure

The prepared structures of the target proteins was loaded to docking software PyRx 0.8 using a load molecule option from the File toolbar. The receptor structure then converted to AutoDock macromolecule (PDBQT format) using the right-click option. Binding affinity studies were performed using Vina Wizard Tool in PyRx 0.8. Molecules (PDBQT Files), both ligands as well as the targets were selected for docking. For molecular docking simulation, the three-dimensional grid box (size_x = −40.697173Ao; size_ y = 33.525519Ao; size_z = −7.529365Ao) for COX-1 (PDB: 3KK6), and (size_x = 30.988577Ao; size_ y = −22.283615Ao; size_z = −16.507231Ao) for COX-2 (PDB: 3LN1) was designed using AutoDock tool 1.5.6 with exhaustiveness value of 8. After selecting molecules, the active amino acid residues were selected to define the cavity with the help of the toggle selection spheres option given in PyRx. To occupy all the active binding sites and essential residues, the grid box was aligned properly. The ligands and targets then subjected for docking to get the finding affinity with each other. First x-ray bound ligand celecoxib was docked against cox1 and cox 2 proteins, and rmsd were calculated to validate the docking protocol. After validation, the same docking protocol was used for further docking with natural products.

2.6. Carrageenan induced paw edema

Wistar rats Male weighing between (160–200 g) were obtained from Wockhardt Ltd, Aurangabad. Animals were housed under standard laboratory condition at a temperature of 25 ± 2 °C, relative humidity of 45–55 percent and standard environmental condition (12 h light and 12 h dark cycles). The animals had free access to standard diet and water. The animals were acclimatized to the laboratory 2 h before the experimentation. Experimental protocol was approved by Animal Ethics Committee (CPCSEA/IAEC/P'cology/71/2020–21/177). The experiment involved inducing paw edema by carrageenan, using the modified procedure previously described by Winter et al. and Sakat et al. [11,15]. The Wistar rats were segregated into distinct groups, each consisting of six individuals, according to their basal paw volume. The induction of inflammation was accomplished by administering a subcutaneous injection of λ-carrageenan, namely 0.1 mL of a 1 % solution in normal saline, into the plantar region of the left hind paw. The paw was inked at the lateral malleolus and its volume was thereafter measured at 1-h intervals for a total of 4 h following the administration of carrageenan to all the animals. These measurements were taken using a digital plethysmometer. In addition, the animals received oral administration of various substances, including a vehicle, Ethyl Acetate Fraction *Chrozophora plicata* [EAFCP] at doses of 100 mg/kg and 200 mg/kg, as well as Indomethacin at a dose of 10 mg/kg, 1 h before to the carrageenan challenge. Paw edema was determined by subtracting the basal paw volume [-1 h] from the corresponding paw volumes at 1 h, 2 h, 3 h, and 4 h. The percentage of anti-inflammatory activity was determined for each animal by employing the subsequent formula: The formula used to calculate the percentage of paw edema in test animals relative to control animals is as follows: [Mean paw edema of test animals in milliliters - Mean paw edema of control animals in milliliters] divided by Mean paw edema of control animals in milliliters, multiplied by 100. The percentage of anti-inflammatory action was determined for each animal by employing the subsequent formula: [Mean paw edema of control animals [ml] - paw edema of each test animal [ml].

2.7. Statistical data

The data was presented in the form of the mean value plus or minus the standard error of the mean [SEM] for each respective group. The statistical analysis was conducted using GraphPad Prism version 5.0 software. The statistical analysis employed in this study involved the utilization of a two-way analysis of variance [ANOVA], followed by Bonferroni post hoc multiple comparison tests. This approach was employed to assess the presence of statistical differences in the carrageenan-induced paw edema test. A significance level of $p < 0.05$ was deemed to indicate statistical significance.

3. Results and discussion

3.1. Phytochemical network and Disease-Target Network

The investigation involved analyzing the signalling pathway and role of specific target genes. Data were processed using Cytoscape software to generate a compound-target network. Fig. 1 illustrates the compound-target-disease interaction network, providing

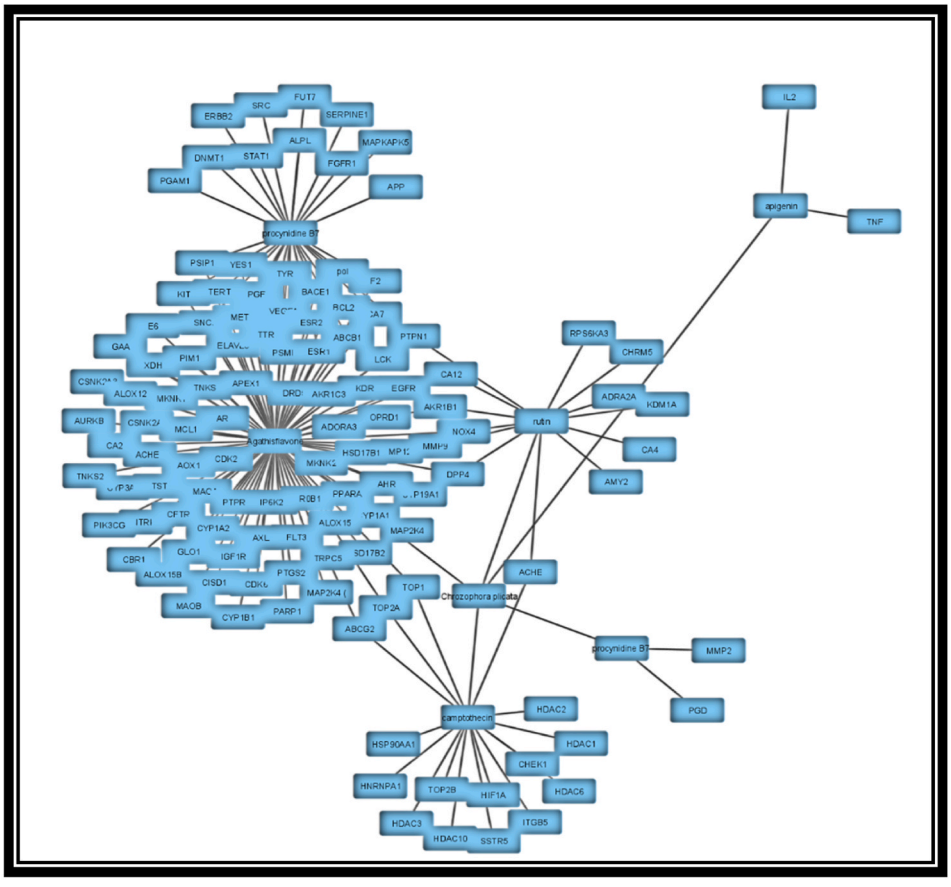

A

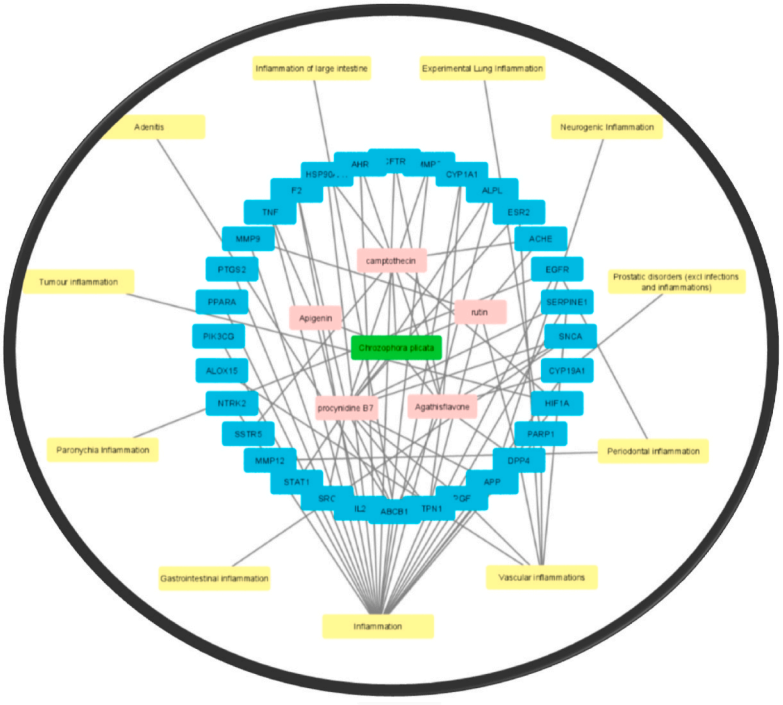

B

(caption on next page)

Fig. 1. Network of Target genes and abundant compounds present in *Chrozophora plicata*,
A. The network was made by filtering the active compounds from the LCMS/QTOF data and appropriate targets for the following compounds from Binding. db database and swissTarget Prediction, each edge represents an interaction with the following connected node.
B. This network shows relationship between the Target nodes and Diseases related to inflammation, data was retrieved from disgenet.com, and gene cards. All of the following network were created in Cytoscape v.11.0.6.

insights into the mechanisms underlying drug efficacy in treating inflammation. This network comprises five ingredients and 155 interactive target proteins. Analysis revealed that numerous targets were affected by multiple components. This suggests that the active biochemical elements of CP potentially exert a synergistic influence on these targets, contributing to its therapeutic efficacy in addressing not only inflammation but also other associated diseases and disorders. Fig. 1A specifically depicts the Disease-Target Network.

Spectra of compound	Structure	ADME	RT	Mass
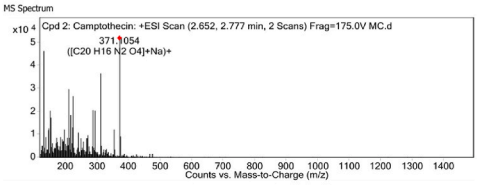	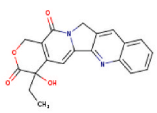		2.2729	348.1162
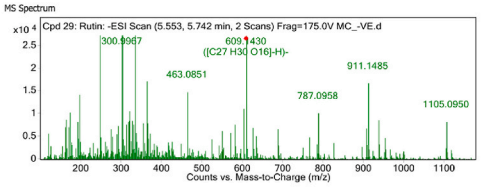	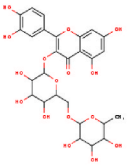	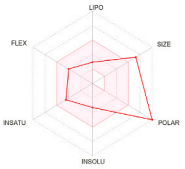	5.6373	610.1504
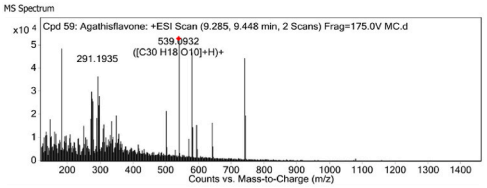	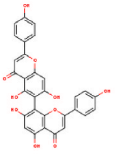		9.381	538.0861
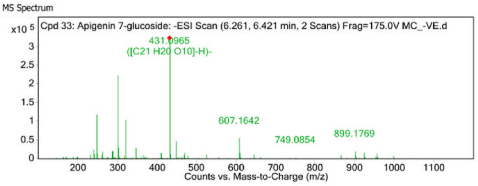	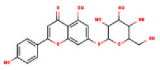		6.357	432.1036
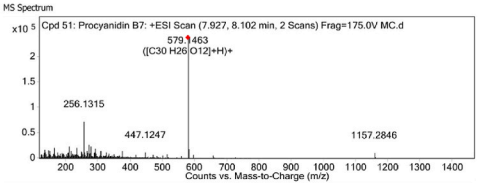	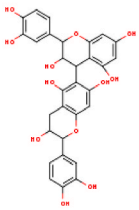	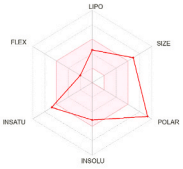	9.04	578.1389

Fig. 2. LCMS QTOF Spectra of each Compounds used in Analysis.

3.2. Phytochemical analysis revealed many phytochemical constituents present in Chrozophora plicata

Based on our prior experiments, we have demonstrated that *C. Plicata* is predominantly comprised of flavonoids. Therefore, we used ethyl acetate extract for LCSM QTOF analysis to elucidate and verify the quantity of flavonoids present in the plant. Using LCMS QTOF, we confirmed that the ethyl extract contained numerous compounds. However, we specifically identified five compounds that were most abundant and also found to have significant therapeutic activity based on a brief review of relevant literature and LCMS QTOF

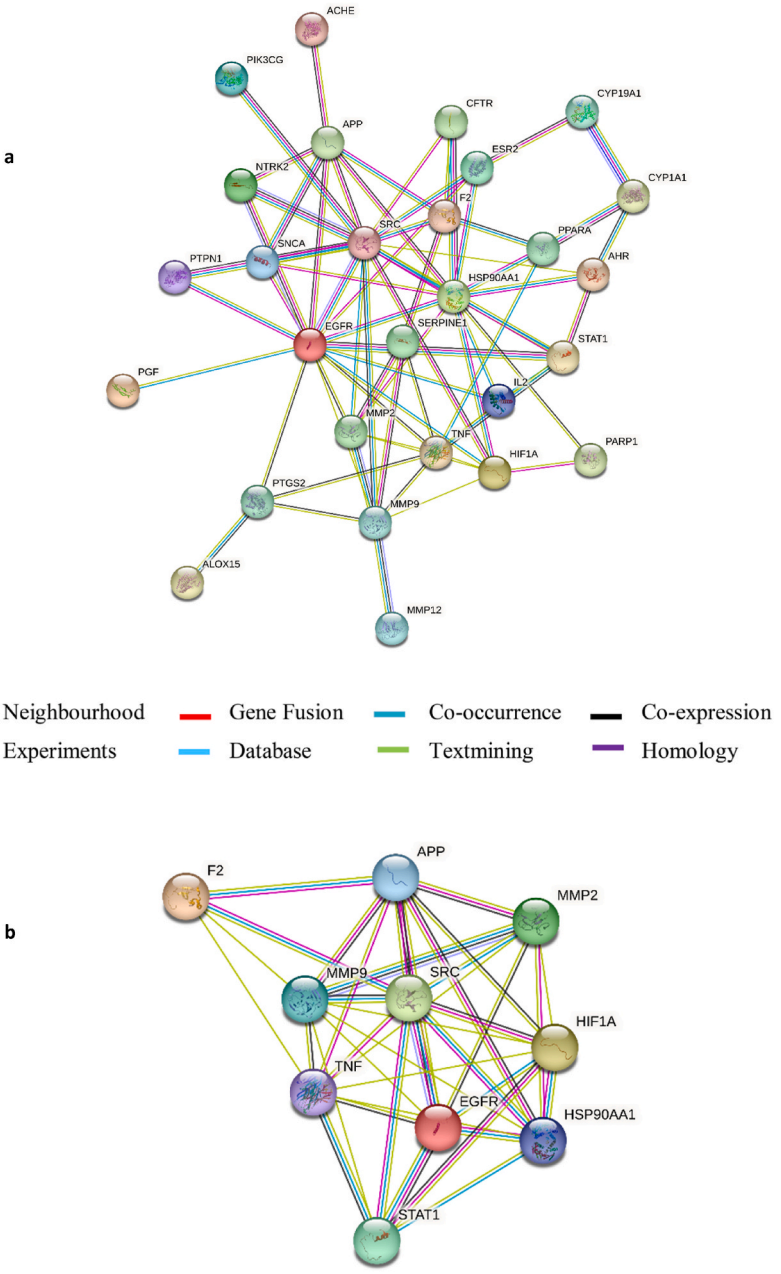

Fig. 3. Protien Interaction Network of Target Genes.
A.Target Genes suspected to be related to inflammation in the Plant extract, 32 Target Nodes were fed into the String Database for PPI network Creation, the rest of the disconnected nodes were deleted. Each Edge represents a protien interaction, each coloured edge represents different types of interactions within the same connected nodes the Network has 28 nodes and 70 edges with an average degree of 5 with p value of 1.0×10^{-16}
B. A smaller PPI network of top 10 tightly clustered and core targets was constructed, which revealed that this sub cluster carried more than half of the total edges in the original network, showing that these 10 target nodes majorly contribute to mediation of Inflammation these were constructed in String Database v11.5.

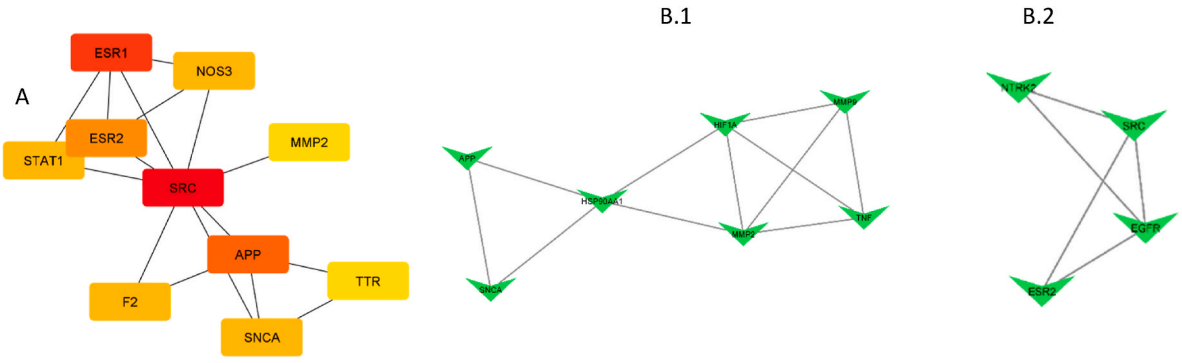

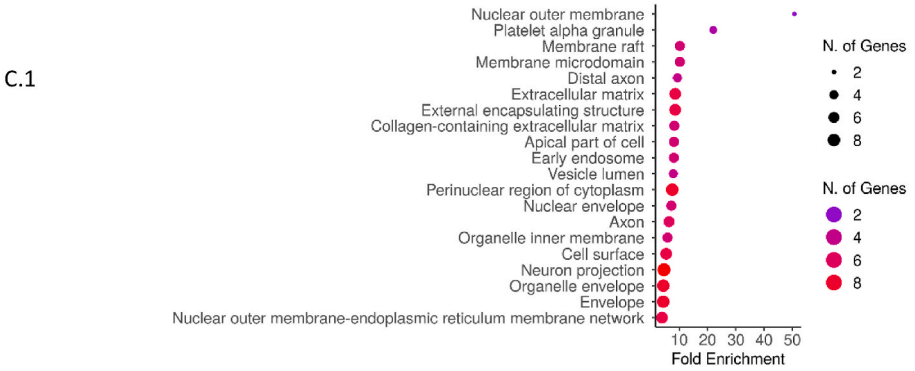

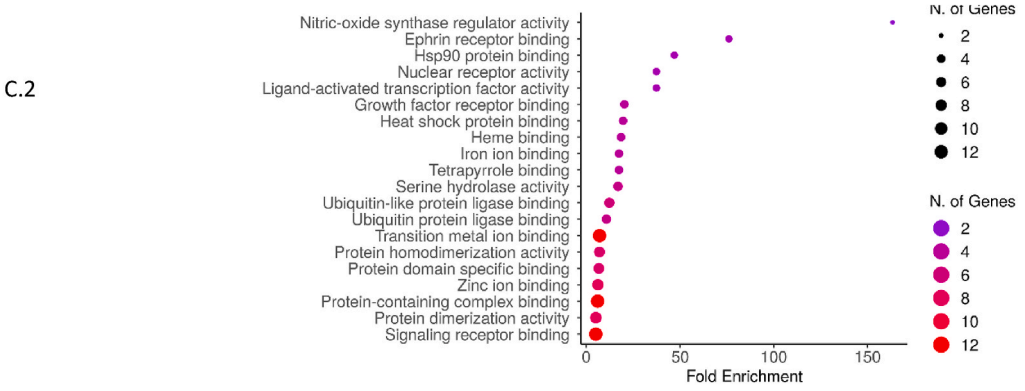

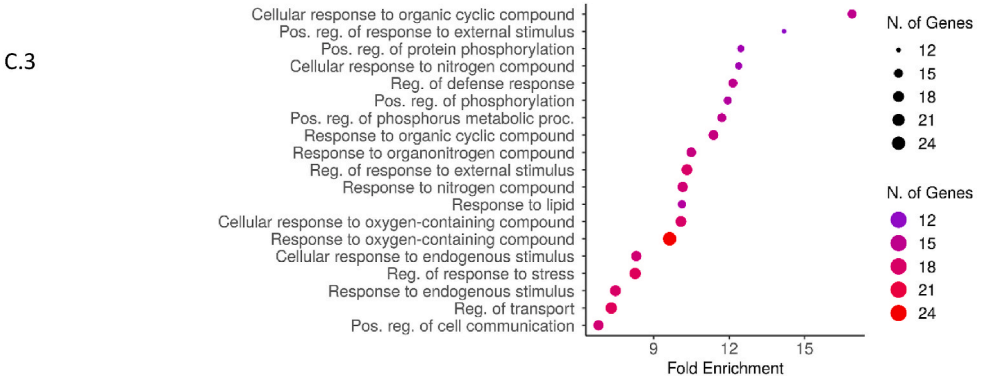

(caption on next page)

Fig. 6. Gene Enrichment Analysis through CytoHubba, MCODE
A. This is a network of Top 10 target genes ranked by Degree obtained by Cytohubba plugin in cytoscape.
B. Sub Clusters Containing highly enriched genes identified in the network through MCODE analysis in Cytoscape. B1. Sub cluster 1 [major], B2. Sub cluster 2 [Minor]
C1. Cellular Component**, C2**. Molecular Function, **C3**. Biological Process,
In these dots plot the darker shade of purple indicates higher enrichment of the process and a larger diameter of the dot indicates a higher number of associated target genes, the X axis is fold enrichment and the Y axis is Respective processes.

data (Fig. 2). These five compounds were Apigenin-7-Glucoside (CID 5385553), Rutin (CID 5280805), Procyanidin B7 (CID 13990893), Camptothecin (CID 24360) and Agathisflavone (CID 5281599). Based on the presence of literature indirectly linking each compound to inflammation, we hypothesized that the collective action of these five compounds would result in an anti-inflammatory effect.

3.3. PPI network of phytochemicals reveals a variety of biological processes this extract regulates

In order to comprehend and forecast the activity of these five phytochemicals when combined, our objective was to generate multiple redundant outcomes through various analyses, thereby providing strong evidence to support the decision to proceed with the hypothesis.

Initially, we constructed a protein-protein interaction (PPI) network using the target genes of *C. plicata* that are linked to inflammation. The PPI Network of target genes related to inflammation was created with a total node of 32 and disconnected nodes were deleted. The final PPI network had 28 nodes with an average degree value of five and 70 edges with a P value $< 1 \times 10^{-16}$ [Fig. 3A]. To analyse the PPI network, we imported it into cytoscape, through an undirected network analysis we determined degree, closeness and centrality which correlate with the role of phytochemical in the total combined action of anti-inflammatory effect, the PPI network was then further analysed through cytohubba plugin in cytoscape to identify top 10 genes with regard to degree in the network [Fig. 6]. The genes were found as follows EGFR, SRC, HSP90AA1, TNF, MMP9, HIF1A, APP, MMP2, STAT1, and F2. EGFR had the highest degree in the PPI Network [Tables 2–3]. A second PPI network was created for the main targets (top 10 genes), revealing a higher number of interactions that were statistically significant [$p < 0.05$]. The PPI network consisted of 38 edges [Fig. 3B]. The core target network had a greater proportion of edges compared to the entire PPI network, with a clustering coefficient of 0.906.

The identified genes exhibited enrichment in various biological processes, including the response to oxygen-containing compounds [GO:1901700], the response to organic substances [GO:0010,033], and the cellular response to organic substances [GO:0071,310]. Additionally, these genes were found to be particularly enriched in cellular components such as transition metal ion binding [GO:0046,914], signalling receptor binding [GO:0005102], identical protein binding [GO:0042,802], the perinuclear region of the cytoplasm [GO:0048,471], and the extracellular space [GO:0005615]. As The Second PPI had more than half edges as compared to the original PPI, and the Biological Processes were related to inflammation, this gave us confidence that these 10 genes must major play a role in inflammation thus providing to our hypothesis of *C. plicata's* anti inflammatory effect, thus we further proceeded to gene enrichement analysis for these 10 genes.

3.4. Gene Enrichment Analysis identifies potential drug action pathways

The Cluego software was employed to investigate the process of gene enrichment across many categories, including biological processes, cellular components, molecular functions, and KEGG pathways [Fig. 4A]. Our compound was discovered to mediate a variety of pathways such as oestrogen signalling pathway, the IL-13, 1L-4, IL-17 pathway, positive regulation of protein kinase b signalling, vascular endothelial growth receptor pathway, signalling in PTK6, and lastly pathways in cancer [Fig. 4A]. All of these signalling pathways imply that the plant extract Regulates intermediary pathways of inflammation while it also interacts strongly with cytokine production during inflammation for example it interacts with IL-4, IL-13 signalling which again impairs the inflammatory response. Another Gene Enrichment Analysis was done through KEGG pathway analysis in Shiny GO (http://bioinformatics.sdstate.edu/go/) were also carried out for more detailed gene ontology graph portraying KEGG pathways providing redundancy in results

Table 2
Top 10 genes in network ranked by degree.

Rank	Name	Degree
1	EGFR	15
1	SRC	15
3	HSP90AA1	13
4	TNF	9
5	MMP9	8
6	HIF1A	7
6	APP	7
6	MMP2	7
9	STAT1	6
10	F2	5

Table 3
Top ten genes ranked by Closeness.

Rank	Name	Degree
1	EGFR	20.83333
1	SRC	20.83333
3	HSP90AA1	19.66667
4	TNF	17.33333
5	MMP9	17
6	HIF1A	16.33333
6	APP	16.33333
6	MMP2	16.33333
9	STAT1	15.83333
10	ESR2	14.83333

through different databases. Through that set of genes it was discovered that our compound can also be used in a variety of diseases like bladder cancer, prostate cancer, diabetic cardiomyopathy, ovarian steroidogenesis etc [Fig. 5].

The Top Ten genes associated with PPI network had great connection to mediating inflammation. The most important gene was Tumour necrosis factor [TNF] which has a crucial function in regulating both acute and chronic inflammation, rendering it one of the most prominently enriched genes within the PPI network. TNF activates the nfKb pathway and AP-1, it often exacerbates acute inflammation when it is inhibited. Moreover, TNF contains two different kinds of receptors, primarily TNFR1 and TNFR2, with TNFR1 exhibiting more significant inflammatory effects [17]. Additionally, when TNF factors are present for a longer period of time, it induces dysregulation in the metabolism of lipids and glucose, which in turn causes proarethrogenic lipid changes. In chronic inflammatory diseases proaretheogenic lipid patterns have been found to be most frequently associated with these diseases, including rheumatoid arthritis a major disease associated with Inflammation [16–19].

Other highly enriched genes in the network are STAT1, HSP90AA1, and SRC which all play a role in inflammation. HSP90AA1 has been demonstrated to be a significant gene for autophagy regulation as some studies show that it promotes autophagy by interacting with mTOR/AKT signalling and NF-xB pathway which consequently leads to inflammation [20–25]. The Literature for all five phytochemicals also links it to inflammation. For instance, Rutin has been demonstrated to regulate inflammation and uphold homeostasis in numerous inflammatory conditions. The primary mode of operation involves diminishing the production of inflammatory agents, such as TNF and NF-kB, which further confirms our findings in network pharmacology [26–29]. Apigenin has demonstrated the ability to reduce inflammation primarily by inhibiting the NF-kB pathway, thereby suppressing COX-2 signalling and the production of inflammatory cytokines such as IL-6, IL-8, and others. Research on plant extracts containing apigenin has demonstrated both anti-inflammatory and anti-cancer properties [30–33]. Camptothecin has demonstrated efficacy in inhibiting multiple inflammation-related pathways, including MAPK, TNF, AKT1, and IL-8 pathways, which have shown resistance to other intervention [34,35]. The consistency between our findings and those of other investigations on these phytochemicals established a high level of confidence in our hypothesis that the botanical extract derived from C. plicata possesses the potential to mitigate inflammation. This provided us with the assurance to conduct molecular docking in order to validate its activity prior to proceeding with in vivo experiments.

3.5. Gene enrichment also revealed the potential for drug usage in many cancers

Kegg Pathway Analysis revealed that the Plant extract might have great potential in many diseases, especially cancer. Literature survey on the genes associated our PPI network confirmed this hypothesis. Inflammatory mediators like TNF-a and IL-1B as well as MMP9 play an important role in increasing the invasiveness of breast cancer when overexpressed [36,37]. By binding with CCN2/CTGF and causing downstream signalling pathway activation and fibrosis, EGFR also contributes to renal inflammation and promotes tumorigenesis in general [38–40]. It also interacts with TNF and becomes transactivated, further providing evidence for the tight junction of TNF and EGFR in the second PPI network [Fig. 3]. The SRC kinase is activated by pro-inflammatory cytokines, and after being activated in tumour cells, it also produces cytokines like TNF-a, and other interleukines which then activates SRC hence promoting inflammation and cancer. The overexpression of this gene has been associated with the initiation and advancement of various types of malignancies [41–43]. In the context of cardiac ischemic reperfusion damage, a study revealed that animals lacking the Toll-like receptor 4 [TLR4] gene had a diminished inflammatory response compared to mice with the wild type TLR4 gene during cardiac reperfusion injury. Significantly lower levels of key factors known to induce an inflammatory response, namely IL-6, IL-1, and TNF-a, were observed. This demonstrates that TLR4 was crucial in the control of inflammatory mediators [44–46]. The gene ALOX15 also interacts with PPARv, which are crucial players in the development of various tumours and the induction of inflammation [47–49]. ALOX15 influences STAT3 signalling and IL-6 expression and by suppressing them to reduce tumour progression and development in colonic epithelial cells. F2, commonly referred to as thrombin or prothrombin, is recognized not only for its involvement in the coagulation cascade but also for its ability to initiate inflammation via cell adhesion [50,51]. Thus, this literature and data review provides prospects for future research into the potential of this plant extract to combat cancer.

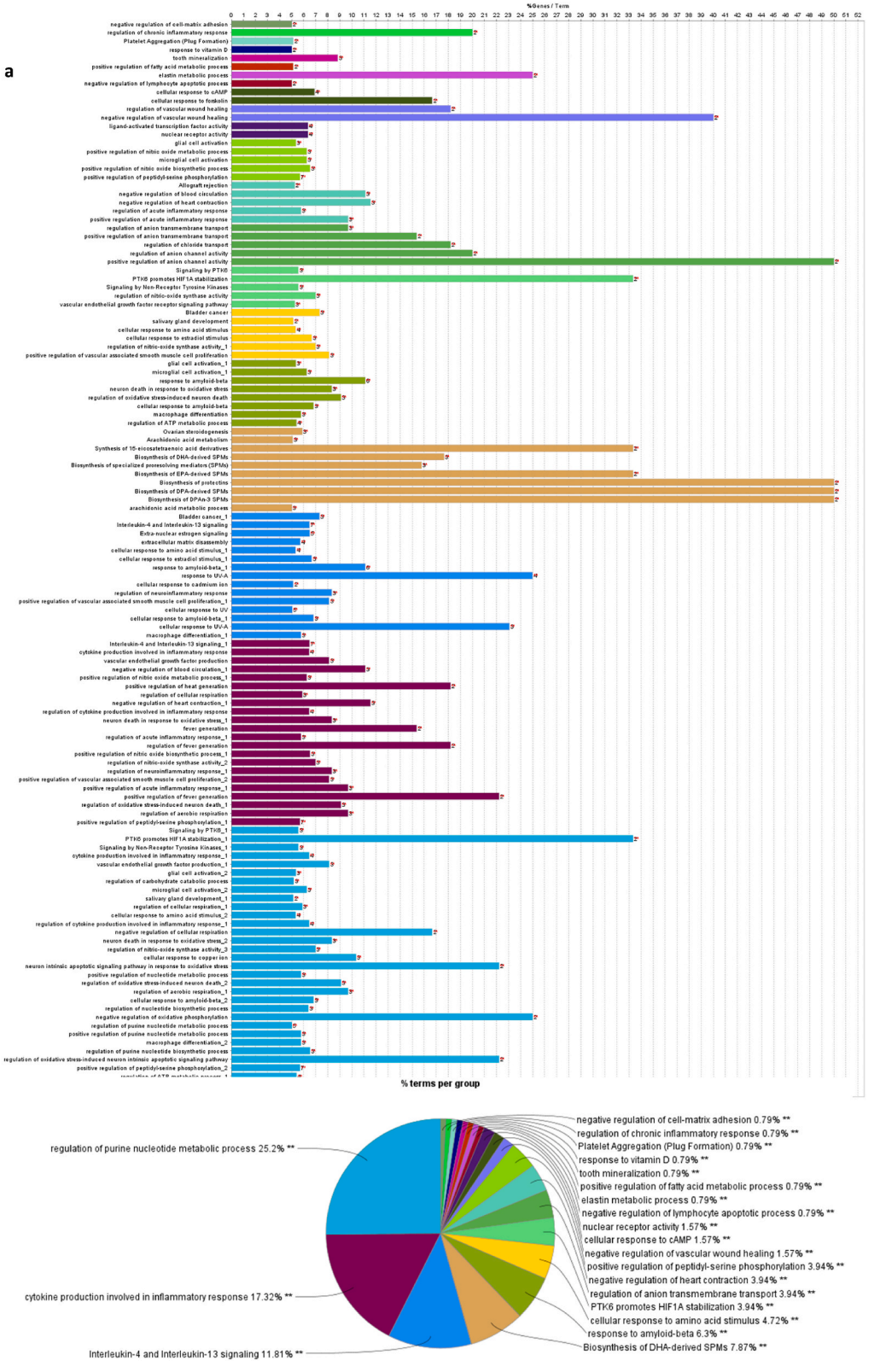

(caption on next page)

Fig. 4. Gene Enrichment Analysis in Cluego.
A. Pathways from the Kyoto Encyclopaedia of Genes and Genomes identifying the biological processes and molecular pathways connected to the following target genes.
B. Pie Chart of the Major Process Types and the % of the Groups Involved.

3.6. Molecular docking analysis

The docking protocol was validated by removing the x ray bound ligand from the complex, re-docking and calculating root mean square deviation (RMSD value) between the docked conformation of the inhibitor and x ray bound conformation as depicted in Fig. 7A and B. The validated protocol was then used for further docking. The selected ligands were successfully docked on the targets to determine their binding affinity (kcal/mol) Table 4 represents the name of the compounds, binding affinity (kcal/mol), and the interacting residues. Binding pose of ligands with receptor was represented in Fig. 8A and B. Molecular docking studies indicated that estimated free energy of binding of docked ligand ranged between −7.4 and −10.4 for COX-1 and -7.3 to −10.3 for COX-2. The binding models between the compounds and proteins have been explained by hydrophobic interaction, hydrogen bond formation and other interactions such as π-Stacking and formation of Salt Bridges. The results indicated that Procyanidine and Apigenin has shown the highest affinity among the series for COX-1 & COX-2 receptors respectively. Further analyses of docking score showed that the binding energy of Procyanidine was −10.4 kcal/mol towards COX-1 compared with standard Indomethacin with binding energy −7.4 kcal/mol with interacting amino acid residues like GLU347, PHE356, GLN358, THR94, ARG109, GLN358, PHE580 and HIS581 amino acid residues as compared to the standard as depicted in Table 4. Moreover, the binding energy of Apigenin towards COX-2 was −10.3 kcal/mol with interacting amino acid residues like GLN178, HIS337, PHE566, ASP333, GLN336 and ASN567 as shown in Table 2. Our docking results are aligned with the in vivo results where all NP have shown good percentage of inhibition as well as showed good binding energies in *in silico* results.

3.7. Ethyl acetate fraction Chrozophora plicata reduces inflammation In-vivo

Subsequently, we proceeded with in-vivo research in order to empirically examine the inflammatory response, thereby validating our computer predictions. In this study, we employed carageenan-induced paw edema models to investigate the effects of the Ethyl Acetate Fraction of *Chrozophora plicata* [EAFCP] at a dosage of 100 and 200 mg/kg administered orally. Our findings revealed a statistically significant reduction in paw edema at 2 h, 3 h, and 4 h [$p < 0.01$] following the administration of EAFCP. In contrast to EAFCP, which shown maximal anti-inflammatory activity of 26.13 %, 21.54.4 %, and 24.65.9 % at 2 h, 3 h, and 4 h, respectively, Indomethacin at a dosage of 10 mg/kg consistently displayed significant [$p < 0.01$] anti-inflammatory effects [>50 %] at all measured time points [Fig. 9A].

The administration of the *Chrozophora plicata* Ethyl Acetate Fraction at a dosage of 200 mg/kg orally resulted in a statistically significant reduction in paw edema at both the 2-h and 3-h time points [$p < 0.05$ & $p < 0.01$]. The paw edema measurements recorded were 0.680.06 ml and 0.970.11 ml, respectively, as illustrated in Fig. 9B. The Ethyl Acetate Fraction had the most significant anti-inflammatory activity at 2 h and 3 h, with respective percentages of 29.3 % and 7.9 %, and 28.0 % and 10.0 %. Furthermore, the IND administered at a dosage of 10 mg/kg exhibited notable anti-inflammatory activity [>50 %] at all-time points, with statistical significance [$p < 0.01$]. The paw edema model is a commonly employed and dependable method for evaluating the anti-inflammatory effects of different substances [52,53]. In the initial stage of inflammation [0–2 h], histamine, 5-hydroxytryptamine, and bradykinin play significant roles as mediators, while the late accelerating phase [after 2 h] is characterized by increased production of COX-2 and prostaglandins [54,55]. Both steroidal and non-steroidal anti-inflammatory medicines [NSAIDs] have been found to have a significant impact on the second phase, as demonstrated by Oates et al. [56]. Acute inflammation is predominantly initiated by prostaglandins. This suggests that EAFCP possesses an anti-inflammatory substance or a combination of substances that hinder the synthesis of prostaglandins and the subsequent inflammatory cascade. In experiments, doses of EAFCP at 100 mg/kg and 200 mg/kg exhibited significant suppression of both the early and late stages of carrageenan-induced inflammation. This effect was achieved by impeding the release of various inflammatory mediators that disrupt the cyclooxygenase pathway.

4. Conclusion

This study scientifically investigates the pharmacological mechanism of CP in the treatment of inflammation through network pharmacology, docking analysis and in vivo animal study. It is in addition worth mentioning that network pharmacology has great advantages in clearing up the mechanism of CP.

Data availability

The Files for network and Molecular docking can requested to mukhtarpharma@gmail.com or reach out to Y·B Chavan college of Pharmacy, Dr Rafiq Zakaria campus Aurangabad 431,001, Maharashtra, India.

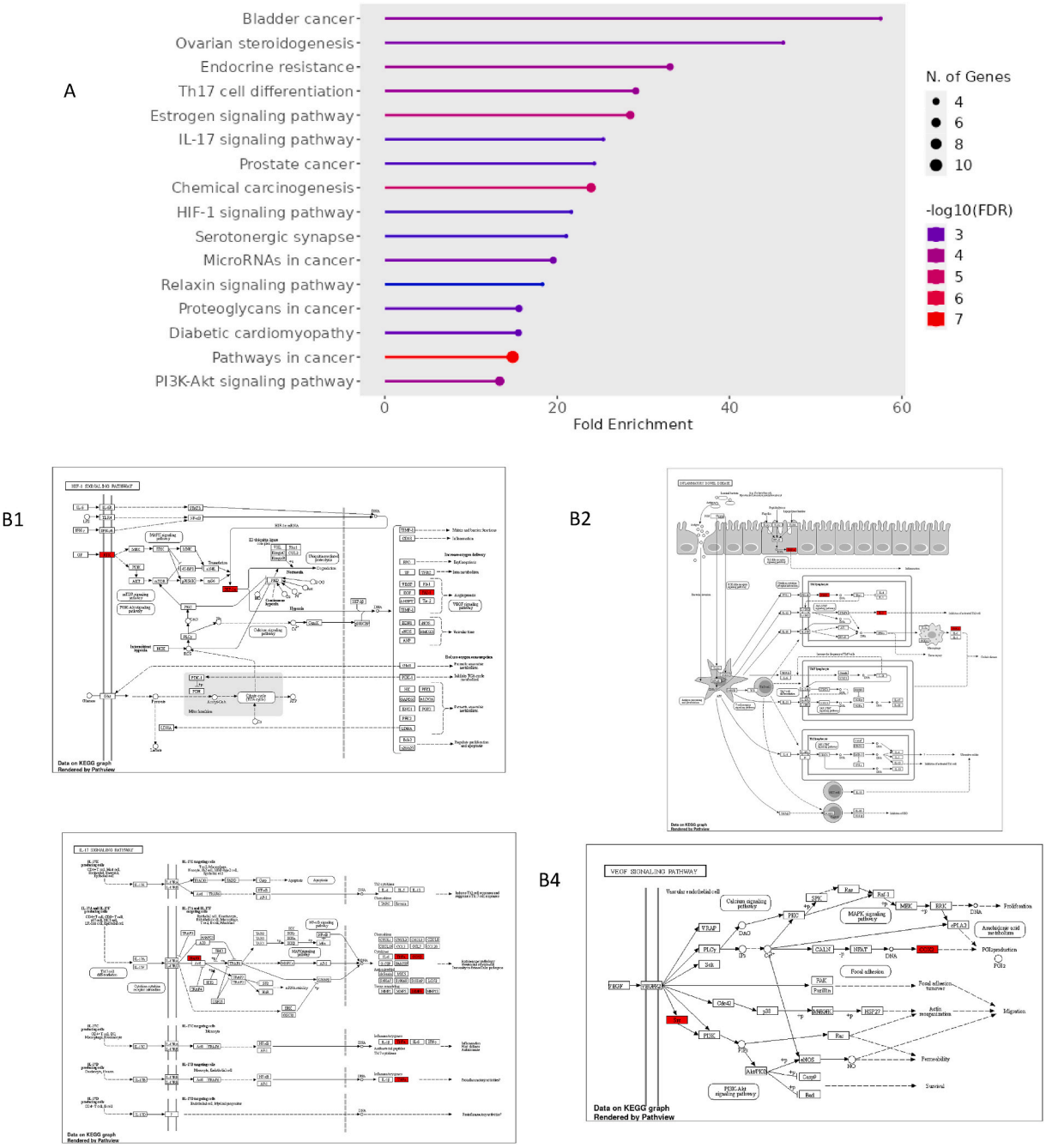

Fig. 5. Gene Enrichment Analysis in KEGG Pathways

A. Lollipop Bar Plot of KEGG pathways Associated with Target genes, the length of the bar plot determines fold enrichment, the larger lollipop at the end of the bar plot represent increasing amount of genes associated with that pathway.

B. Target Genes are Highlighted red in Pathology of different Pathways/diseases and Mediator Release.

B1, HIF1 pathway,

B2. Irritable Bowel Syndrome,

B3. IL-17 pathway,

B4. VEGF signalling pathway.

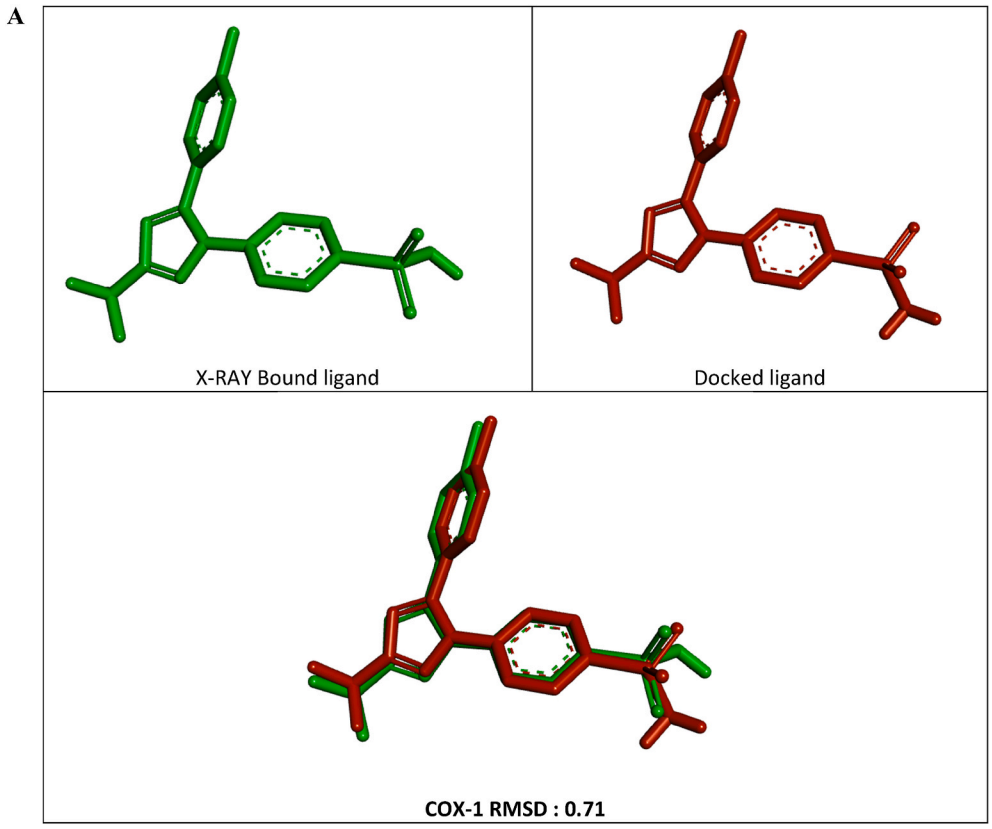

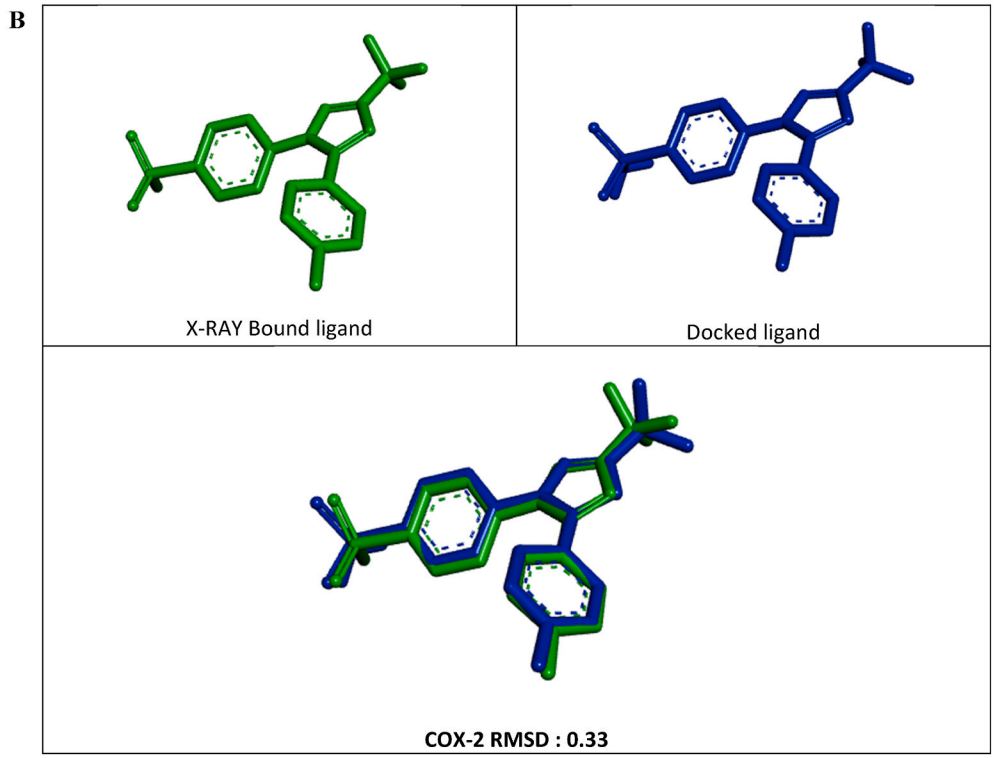

Fig. 7A. RMSD value between X-RAY Bound ligand & Docked Ligand of COX-1 receptor (PDB ID: 3KK6)
Fig. 7B RMSD value between X-RAY Bound ligand & Docked Ligand of COX-2 receptor (PDB ID: 3LN1).

Table 4
Estimated Free Energy of Binding, interacting residues and Number of H bonding between compounds and receptors.

Targets	Complex (protein-Ligand)	Binding Affinity	Interacting Residues	No. of H bonds
3KK6	Agathisflavone	−9.9	THR94,GLN192,PHE356,ASN515,HIS90,HIS581	6
	Apigenin	−9.9	THR94,PRO514,ASN515,GLN192,GLN351,SER353	6
	Camptothecin	−8.8	THR94,PHE356,ASN515, HIS95, SER353	2
	Procyanidine	−10.4	GLU347,PHE356,GLN358,THR94,ARG109,GLN358,PHE580,HIS581	7
	Rutin	−9.2	ILE89,LEU93,VAL349,LEU352,TYR355,PHE518,ILE523,ALA527,HIS90,SER530,LEU531, ARG120	6
	Indomethacin	−7.4	VAL116,VAL349,LEU359,ILE523,ALA527,PHE518	3
3LN1	Agathisflavone	−10.1	VAL75,LEU78,TYR101,VAL102,LEU338,TYR341,LEU345,PHE504,VAL509,ALA513,HIS75, ARG106,TYR341,TYR371,VAL509,SER516,LEU517	8
	Apigenin	−10.3	GLN178,HIS337,PHE566,ASP333,GLN336,ASN567	4
	Camptothecin	−8.3	VAL102, VAL335, TYR341, ALA502, ILE503, PHE504, VAL509, LEU517, SER516	2
	Procyanidine	−9.6	GLN336,THR79,ASP333,HIS337	6
	Rutin	−9.3	GLN337,SER565,PHE566,ASN567,HIS337	3
	Indomethacin	−7.3	TYR341, PHE504, LEU338, MET508, GLY512, SER516	4

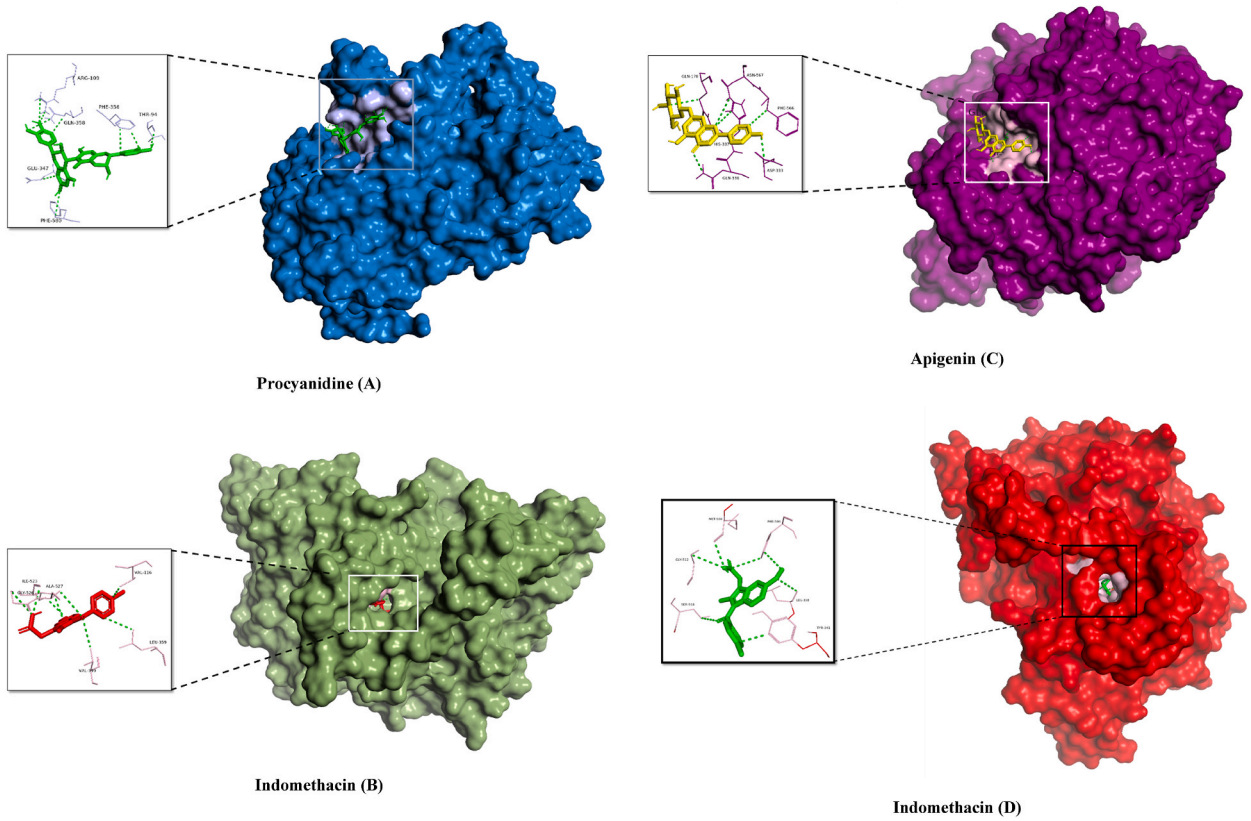

Fig. 8A. 3D docking pose of Procyanidine (A) and Indomethacin (B) with COX-1 (PDB: 3KK6)
Fig. 8B 3D docking pose of Apigenin (C) and Indomethacin (D) with COX-2 (PDB: 3LN1).

CRediT authorship contribution statement

Mohd Mukhtar Khan: Writing – review & editing, Writing – original draft, Resources, Methodology, Investigation, Formal analysis, Data curation, Conceptualization. **Md Affan Shaikh:** Software. **Yasar Qazi:** Visualization. **Subur W. Khan:** Investigation, Formal analysis. **Syed Ayaz Ali:** Writing – review & editing, Supervision, Methodology, Conceptualization.

Declaration of competing interest

The authors declare the following financial interests/personal relationships which may be considered as potential competing

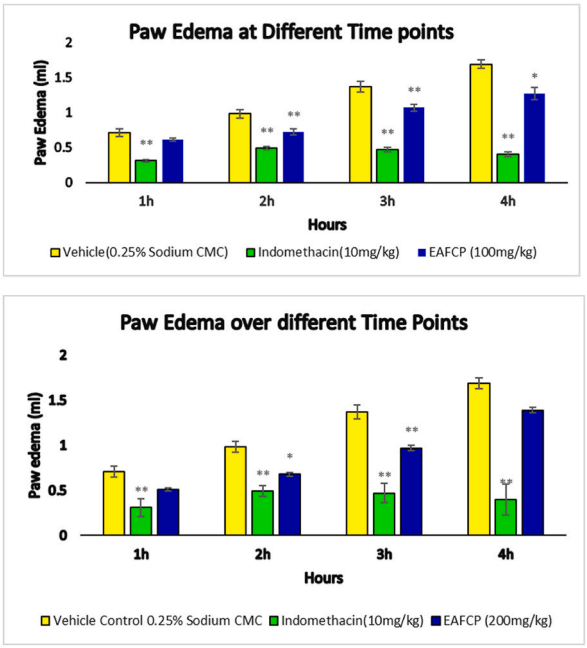

Fig. 9A. Effect of vehicle, EAFCP [100 mg/kg] and Indomethacin [IND 10 mg/kg] on carrageenan induced paw edema. Values in the results are expressed as mean ± SEM, [n = 6], *p < 0.05, **p < 0.01 significantly different in comparison to vehicle control at respective time points, **B.** Effect of vehicle, EAFCP [200 mg/kg] and Indomethacin [IND 10 mg/kg] on carrageenan induced paw edema. Values in the results are expressed as mean ± SEM, [n = 6], *p < 0.05, **p < 0.01 significantly different in comparison to vehicle control at respective time points.

interests:Mohd Mukhtar Khan reports a relationship with Maulana Azad Educational Trust's Y B Chavan College of Pharmacy that includes: employment.

Acknowledgements

The authors thankful to the Maulana Azad Educational Trust, Dr. Rafiq Zakaria Campus, and Y. B Chavan College of pharmacy, Aurangabad 431001(MS), India for providing the laboratory facility. Authors are also thankful to IIT Powai, Mumbai for providing the compound analysis. Authors are also thankful to Dr. Nafees Ahemad, Monash University, Malaysia.

Appendix A. Supplementary data

Supplementary data to this article can be found online at https://doi.org/10.1016/j.heliyon.2024.e24617.

References

[1] L. Chen, H. Deng, H. Cui, J. Fang, Z. Zuo, J. Deng, et al., Inflammatory responses and inflammation-associated diseases in organs, Oncotarget 9 (6) (2017 Dec) 7204–7218.
[2] D. Furman, J. Campisi, E. Verdin, P. Carrera-Bastos, S. Targ, C. Franceschi, et al., Chronic Inflammation in the Etiology of Disease across the Life Span, s. vols. 1822–1832, Nature Portfolio, 2019.
[3] A.L. Hopkins, Network pharmacology: the next paradigm in drug discovery, Nat. Chem. Biol. 4 (11) (2008 Oct) 682–690.
[4] C.A. Winter, E.A. Risley, G.W. Nuss, Carrageenin-induced edema in hind paw of the rat as an assay for antiinflammatory drugs, Exp. Biol. Med. 111 (3) (1962 Dec) 544–547.
[5] F. Noor, M. ul Qamar, U.A. Ashfaq, A. Albutti, A.S.S. Alwashmi, M.A. Aljasir, Network pharmacology approach for medicinal plants: review and assessment, Pharmaceuticals 15 (5) (2022 May) 572.
[6] L. Yang, Y. Zhao, H. Xu, Y. Ma, L. Wang, J. Ma, et al., Network pharmacology-based prediction and verification of the potential mechanisms of hes yangchao formula against diminished ovarian reserve, in: S. Yang (Ed.), Evidence-Based Complementary and Alternative Medicine, 2022, pp. 1–16, 2022 Jun.
[7] H. Maurya, M. Semwal, S.K. Dubey, Pharmacological evaluation of Chrozophora tinctoria as wound healing potential in diabetic rats model, BioMed Res. Int. 2016 (2016) 1–7.
[8] G. Stelzer, N. Rosen, I. Plaschkes, S. Zimmerman, M. Twik, S. Fishilevich, et al., The GeneCards suite: from gene data mining to disease genome sequence analyses, Curr Protoc Bioinformatics 54 (1) (2016 Jul).
[9] M. Mohammed, Y. Kadil, I. Rahmoune, H. Filali, Exploration of novel PDEδ inhibitor based on pharmacophore and molecular docking against KRAS mutant in colorectal cancer, Curr. Drug Discov. Technol. 20 (4) (2023 Sep).
[10] N.S. Sakle, S.A. More, S.N. Mokale, A network pharmacology-based approach to explore potential targets of Caesalpinia pulcherima: an updated prototype in drug discovery, Sci. Rep. 10 (1) (2020 Oct).

[11] N.S. Sakle, S.A. More, S.N. Mokale, A network pharmacology-based approach to explore potential targets of Caesalpinia pulcherima: an updated prototype in drug discovery, Sci. Rep. 10 (1) (2020 Oct).
[12] C.H. Chin, S.H. Chen, H.H. Wu, C.W. Ho, M.T. Ko, C.Y. Lin, cytoHubba: identifying hub objects and sub-networks from complex interactome, BMC Syst. Biol. 8 (4) (2014 Dec 8).
[13] H. Jiang T, J. Xu, Y. Lu, X. Chen, Y. Li, Network Pharmacology Analysis and Experimental Validation to Explore the Anti-inflammatory Mechanism of Asiatic Acid on Alcoholic Steatohepatitis, 2022.
[14] N. Geng, Y.P. Qi, W.W. Qin, S. Li, H. Jin, Y. Jiang, et al., Two microRNAs of Plasma-Derived Small Extracellular Vesicles as Biomarkers for Metastatic Non-small Cell Lung Cancer, vol. 23, Springer Science+Business Media, 2023.
[15] C.A. Winter, E.A. Risley, G.W. Nuss, Carrageenin-induced edema in hind paw of the rat as an assay for antiinflammatory drugs, Exp. Biol. Med. 111 (3) (1962 Dec) 544–547.
[16] J. Bradley, TNF-mediated inflammatory disease, J. Pathol. 214 (2) (2008 Jul) 149–160.
[17] G. van Loo, M.J.M. Bertrand, Death by TNF: a road to inflammation, Nat. Rev. Immunol. 23 (5) (2022 Nov) 289–303.
[18] J. Bradley, TNF-mediated inflammatory disease, J. Pathol. 214 (2) (2008 Jul) 149–160.
[19] C. Popa, M.G. Netea, P.L. van Riel, J.W. van der Meer, A.F. Stalenhoef, The role of TNF-\alpha{ }in chronic inflammatory conditions, intermediary metabolism, and cardiovascular risk, J. Lipid Res. 48 (4) (2007 Jul) 751–762.
[20] M. Zhou, W. Xu, J. Wang, J. Yan, Y. Shi, C. Zhang, et al., Boosting mTOR-dependent autophagy via upstream TLR4-MyD88-MAPK signalling and downstream NF-\kappa{ }B pathway quenches intestinal inflammation and oxidative stress injury, EBioMedicine 35 (2018 Jul) 345–360.
[21] H. Zhang, X. Zhang, J. Huang, X. Fan, Identification of key genes and pathways for peri-implantitis through the analysis of gene expression data, Exp. Ther. Med. 13 (5) (2017 Mar) 1832–1840.
[22] H. Zhang, J. Huang, X. Fan, R. Miao, Y. Wang, HSP90AA1 promotes the inflammation in human gingival fibroblasts induced by Porphyromonas gingivalis lipopolysaccharide via regulating of autophagy, BMC Oral Health 22 (1) (2022 Aug).
[23] B. Staels, W. Koenig, A. Habib, R. Merval, M. Lebret, I.P. Torra, et al., Activation of human aortic smooth-muscle cells is inhibited by PPAR\alpha{ }but not by PPAR\gamma{ }activators, Nature 393 (6687) (1998 Jul) 790–793.
[24] J. Kowalski, B. Okopien, A. Madej, M. Zielinski, D. Belowski, Z. Kalina, et al., Effects of fenofibrate and simvastatin on plasma sICAM-1 and MCP-1 concentrations in patients with hyperlipoproteinemia, Int. J. Clin. Pharm. Ther. 41 (6) (2003 Jun) 241–247.
[25] G. Chinetti, J.C. Fruchart, B. Staels, Peroxisome proliferator-activated receptors (PPARs): nuclear receptors at the crossroads between lipid metabolism and inflammation, Inflamm. Res. 49 (10) (2000 Oct) 497–505.
[26] C. Tian, Y. Chang, Z. Zhang, H. Wang, S. Xiao, C. Cui, et al., Extraction technology, component analysis, antioxidant, antibacterial, analgesic and anti-inflammatory activities of flavonoids fraction from Tribulus terrestris L. leaves, Heliyon 5 (8) (2019 Dec) e02234.
[27] J.H. Chen, C.L. Zhao, Y.S. Li, Y.B. Yang, J.G. Luo, C. Zhang, et al., Moutai Distiller's grains Polyphenol extracts and rutin alleviate DSS-induced colitis in mice: modulation of gut microbiota and intestinal barrier function (R2), Heliyon 9 (11) (2023 Dec) e22186.
[28] S. Nafees, S. Rashid, N. Ali, S.K. Hasan, S. Sultana, Rutin ameliorates cyclophosphamide induced oxidative stress and inflammation in Wistar rats: role of NF \kappa{ }B/MAPK pathway, Chem. Biol. Interact. 231 (2015 Dec) 98–107.
[29] A.Y. Lee, S. Lee, H. Kim, S. Lee, E.J. Cho, Anti-inflammatory effects of luteolin and luteoloside from Taraxacum coreanum in RAW264.7 macrophage cells 747–754 (2016).
[30] M.C. Wang, Natural plant resource flavonoids as potential therapeutic drugs for pulmonary fibrosis, Heliyon 9 (8) (2023 Dec) e19308.
[31] N. Sharma, Radha, M. Kumar, N. Kumari, S. Puri, N. Rais, et al., Phytochemicals, therapeutic benefits and applications of chrysanthemum flower: a review, Heliyon 9 (10) (2023 Dec) e20232.
[32] N. Ngernyuang, M. Wongwattanakul, W. Charusirisawad, R. Shao, T. Limpaiboon, Green synthesized apigenin conjugated gold nanoparticles inhibit cholangiocarcinoma cell activity and endothelial cell angiogenesis in vitro, Heliyon 8 (12) (2022 Dec) e12028.
[33] R. Lim, G. Barker, C.A. Wall, M. Lappas, Dietary phytophenols curcumin, naringenin and apigenin reduce infection-induced inflammatory and contractile pathways in human placenta, foetal membranes and myometrium, MHR: Basic science of reproductive medicine 19 (7) (2013 Mar) 451–462.
[34] D. He, S. Fu, A. Zhou, Y. Su, X. Gao, Y. Zhang, et al., Camptothecin Regulates Microglia Polarization and Exerts Neuroprotective Effects via Activating AKT/Nrf2/HO-1 and Inhibiting NF-\kappa{ }B Pathways in Vivo and in Vitro, vol. 12, 2021.
[35] Y. Wang, K. Liu, Z. Qi, T. Chen, W. Yu, Y. Jiang, et al., Therapeutic mechanism and effect of camptothecin on dextran sodium sulfate-induced ulcerative colitis in mice, in: E. Rigopoulou (Ed.), J Immunol Res (2021) 1–13, 2021 Apr.
[36] X. Wang, Y.Y. Yu, S. Lieu, F. Yang, J. Lang, C. Lu, et al., MMP9 regulates the cellular response to inflammation after skeletal injury, Bone 52 (1) (2013 Jul) 111–119.
[37] G. Chen, X.F. Ding, K. Pressley, H. Bouamar, B. Wang, G. Zheng, et al., Everolimus inhibits the progression of ductal carcinoma in situ to invasive breast cancer via downregulation of MMP9 expression, Clin. Cancer Res. 26 (6) (2020 Mar) 1486–1496.
[38] J. Pourazar, A. Blomberg, F.J. Kelly, D.E. Davies, S.J. Wilson, S.T. Holgate, et al., Diesel exhaust increases EGFR and phosphorylated C-terminal Tyr 1173 in the bronchial epithelium, Part. Fibre Toxicol. 5 (1) (2008 May).
[39] S.S. Hobbs, J.A. Goettel, D. Liang, F. Yan, K.L. Edelblum, M.R. Frey, et al., TNF transactivation of EGFR stimulates cytoprotective COX-2 expression in gastrointestinal epithelial cells, Am. J. Physiol. Gastrointest. Liver Physiol. 301 (2) (2011 Jul) G220–G229.
[40] S. RayegoMateos, J.L. MorgadoPascual, A.B. Sanz, A.M. Ramos, S. Eguchi, D. Batlle, et al., TWEAK transactivation of the epidermal growth factor receptor mediates renal inflammation, J. Pathol. 231 (4) (2013 Nov) 480–494.
[41] E. Spaeth, A. Klopp, J. Dembinski, M. Andreeff, F. Marini, Inflammation and tumor microenvironments: defining the migratory itinerary of mesenchymal stem cells, Gene Ther. 15 (10) (2008 Apr) 730–738.
[42] Y. Fu, R. Zagozdzon, R. Avraham, H. Avraham, CHK negatively regulates Lyn kinase and suppresses pancreatic cancer cell invasion, Int. J. Oncol. (2006 Dec).
[43] S.T. Liu, H. Pham, S.J. Pandol, A. Ptasznik, Src as the link between inflammation and cancer, Front. Physiol. 4 (2014).
[44] N.M. Foley, J. Wang, H.P. Redmond, J.H. Wang, Current knowledge and future directions of TLR and NOD signaling in sepsis, Mil Med Res 2 (1) (2015 Jan).
[45] H. Chen, R.Q. Zhang, X.G. Wei, X.M. Ren, X.Q. Gao, Mechanism of TLR-4/NF-\kappa{ }B pathway in myocardial ischemia reperfusion injury of mouse, Asian Pac. J. Tropical Med. 9 (5) (2016 Jul) 503–507.
[46] H. Chen, R.Q. Zhang, X.G. Wei, X.M. Ren, X.Q. Gao, Mechanism of TLR-4/NF-\kappa{ }B pathway in myocardial ischemia reperfusion injury of mouse, Asian Pac. J. Tropical Med. 9 (5) (2016 Jul) 503–507.
[47] F. Mao, M. Xu, X. Zuo, J. Yu, W. Xu, M.J. Moussalli, et al., 15Lipoxygenase1 suppression of colitisassociated colon cancer through inhibition of the IL6/STAT3 signaling pathway, Faseb. J. 29 (6) (2015 Feb) 2359–2370.
[48] R. Tian, X. Zuo, J. Jaoude, F. Mao, J. Colby, I. Shureiqi, ALOX15 as a suppressor of inflammation and cancer: lost in the link, Prostag. Other Lipid Mediat. 132 (2017 Jul) 77–83.
[49] B. Desvergne, W. Wahli, Peroxisome proliferator-activated receptors: nuclear control of metabolism, Endocr. Rev. 20 (5) (1999 Oct) 649–688.
[50] F.Y.K. Demirci, A.S. Dressen, C.M. Kammerer, M.M. Barmada, A.H. Kao, R. Ramsey-Goldman, et al., Functional polymorphisms of the coagulation factor II gene (F2) and susceptibility to systemic lupus erythematosus, J. Rheumatol. 38 (4) (2011 Jan) 652–657.
[51] N.H. Gehring, U. Frede, G. Neu-Yilik, P. Hundsdoerfer, B. Vetter, M.W. Hentze, et al., Increased efficiency of mRNA 3 end formation: a new genetic mechanism contributing to hereditary thrombophilia, Nat. Genet. 28 (4) (2001 Jul) 389–392.
[52] B. Koti, V. Tikare, A. Viswanathaswamy, P. Ashok, A. Thippeswamy, P. Dabadi, Evaluation of antiinflammatory activity of centratherum anthelminticum (L) kuntze seed, Indian J. Pharmaceut. Sci. 72 (6) (2010) 697.
[53] J. Fernandes, H.M. Spindola, V.P. De Sousa, A. Santos-Silva, M. Pintado, F.X. Malcata, et al., Anti-Inflammatory Activity of Chitooligosaccharides in Vivo, s. vols. 1763–1768, Multidisciplinary Digital Publishing Institute, 2010.

[54] M. Di Rosa, J.P. Giroud, D.A. Willoughby, Studies of the mediators of the acute inflammatory response induced in rats in different sites by carrageenan and turpentine, J. Pathol. 104 (1) (1971 Sep) 15–29.
[55] S. Sakat, K. Mani, Y.O. Demidchenko, E.A. Gorbunov, S.A. Tarasov, A. Mathur, et al., RETRACTED ARTICLE: Release-Active Dilutions of Diclofenac Enhance Anti-inflammatory Effect of Diclofenac in Carrageenan-Induced Rat Paw Edema Model, s. vols. 1–9, Springer Science+Business Media, 2013.
[56] J.A. Oates, A.J. Wood, P.M. Brooks, R.O. Day, Nonsteroidal antiinflammatory drugs — differences and similarities, N. Engl. J. Med. 324 (24) (1991 Jun) 1716–1725.